Analysis of Inverse Snyder Optimizations

Erika Harrison, Ali Mahdavi-Amiri, and Faramarz Samavati

University of Calgary, Calgary AB, Canada

Abstract. Modern area preserving projections employed by cartographers and geographers have closed forms when transitioning between the sphere and the plane. Inversions - from the planar map to the spherical approximation of the Earth - are slower, requiring iterative root finding approaches or entirely undetermined. Recent optimizations of the common Inverse Snyder Equal Area Polyhedral projection have been fairly successful, however the work herein improves it further by adjusting the approximating polynomial. An evaluation against the original and improved optimizations is provided, along with a previously unexplored real-time analysis.

Keywords: equal area, projection, optimization, Snyder projection

1 Introduction

The construction of maps which preserve area has long been discussed within the cartographic community. Such a property is particularly desirable for the scientific community. Researchers exploring migratory or meteorological patterns, disease proliferation and control, and many other fields of study rely on accurate areal and regional information. Even business analysts, exploring optimal market demographics and product distribution benefit from area preserving representations of the Earth. These digital environments act as models, or virtual cyberworlds, upon which important analysis may be performed. As such, when representing their spatially-aware data, it is imperative to preserve area when translating between the spherical and planar maps these cyberworlds maintain.

Traditionally projections transform a point p on the Earth, to a point p' on the map (Figure 1), often preserving a variety of properties. Due to the sphericity of the Earth, area and angle - or shape - are unable to be simultaneously preserved [2]. The objective, then, becomes the absolute preservation of area, while reducing shape distortion. In this way, the resultant data appears to be of the correct form, but guarantees accurate regional calculations. Through the novel use of a polyhedral surface, rather than a flat map, Snyder's [14] polyhedral projection is extremely successful at reducing angular distortion, and has been recommended for equal area projections [8].

The inverse process - transforming from the planar representation to the sphere - is of particular important, especially when working within a digital environment. The visualization process tends to work with the planar maps and

images, but prefers a spherical visualization - as is the case for Google Earth [4]. As a result, the inverse projection becomes particularly important.

Efficiency of both the forward and inverse projection is of extreme importance. For the visualization of a single lake, for example, a thousand points may require projection. If hundreds of lakes are evaluated, over a million points must be transformed. Park boundaries, roads and cities may also be projected - often simultaneously - to meet the needs of businesses, military planners, and scientific researchers. An efficient approach must be taken to meet their real-time needs as motivated by geoscience visualization companies [12]. Consequently, an operationally effective and memory efficient approach for an inverse projection is desired.

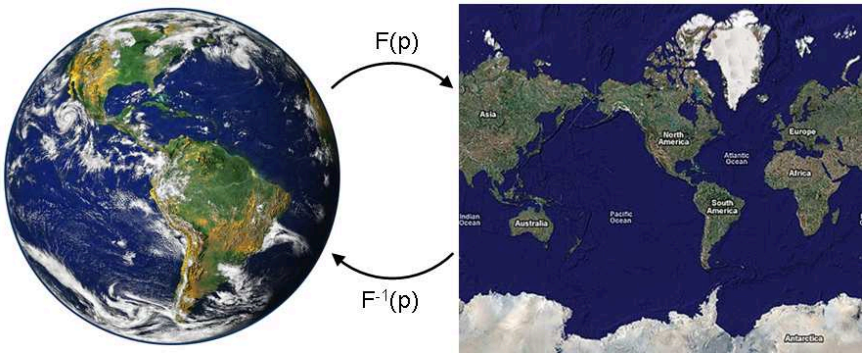

Fig. 1. Projection from the Earth to Planar Map and Inverse (Right: Blue Marble, NASA [11], Left: Mercator Projection, Google Maps [5])

Snyder's equal area approach defines both a forward and inverse projection. His unique approach - employing a polyhedron - and its resultant reduced angular distortion, makes it highly desirable within the modern visualization community. Area is maintained by applying the Lambert Azimuthal Equal Area projection [9] to each of the respective faces, and then adjusted slightly to ensure accurate edge matching. Through a collection of trigonometric equations, function $F(p)$ is defined. Its inverse, $F^{-1}(p)$, is computed by Snyder as a direct reversal of the forward projection. Unfortunately, due to the trigonometric equations, a non-linear system must be solved. Since neither Snyder nor traditional evaluations are able to construct an analytical or closed form, numerical technique is employed.

As a consequence of this non-linear system, the computational time of solving this non-linear system is a large bottleneck. While the closed form of the forward projection has a reliable computation time by calculating each of the equations only once, the numerical technique for finding solutions for the inversion causes an indeterminate number of repeated calculations before converging to a desirable solution. Since these iterations are applied for each of the poten-

tially millions of inverse projection calls, the visualization and analysis process can be immensely impeded.

Few other approaches preserve area, while reducing shape distortion as successfully as Snyder does. Leeuwen et al.'s Slice and Dice projection [10] offer a potential alternative, however it does not define an inverse process, let along a computationally efficient one.

Harrison et al. [7] were able to improve Snyder's inverse process by reducing the iterations to a one dimensional approximating curve. This improved initial estimate reduced the convergence time, while still retaining precise area. An alternative direct replacement of the iterative process with this approximating curve resulted in a 45% faster calculation, with a displacement error of 5.9 m, and areal error of 0.7 km^2. Expanding on this success, we have evaluated alternative approximating curves, and analyzed the real-time improvements.

We start with a brief discussion of the Snyder equal area polyhedral projection, and its inversion. The optimizations from Harrison et al. are reviewed. Our expansions are then discussed. The different polynomial approximating curves are evaluated, a real-time analysis is explored, and finally results are presented accordingly.

2 Background

As computers have improved in power over the years, they have increasingly been incorporated into different fields of study. As late as 1998, former US Vice President, Al Gore proposed a Digital Earth framework [6]. The objective has been to harness the capabilities of computing power to visualize and analyze the Earth's surface directly upon a 3D spherical representation. Consequently, planar input, such as satellite imagery, field surveys and other such 2D data must be transformed into their respective spherical coordinates. While one way to accomplish this is through the employment of accurate Geographic Information System protocol, this is not applicable to large regional input, such as satellite photography. Instead, data must be projected to the appropriate position. These projections, between the planar map and the Earth, range in shape and style, objective and aesthetic, developed continuously over the last two thousand years [15].

These cartographic projections are thereby tasked with overcoming the problems faced with spherical to planar transference. In particular, the inability to simultaneously preserve angle and area results in projections constructed and employed based on the desired qualities of the specific task [2]. Projections are often selected based on the need for preservation of area, preservation of shape, distance and positional accuracy, and an ease of computation [13]. With the prevalence of computers, this ease of computation becomes less critical to cartographers. However, within a Digital Earth framework, requiring immense quantity of data, and a desired real-time analysis, computational complexity remains of high importance.

Researchers and analysts exploring regional-based information, require preservation of area. Equal area projections have been documented since Ptolemy's *Geographia* manuscripts in the second century [15], often incorporating other desirable characteristics. The Werner projection of the 16th century, for example, is able to preserve a collection of longitudinal distances, at the expense of severe shape distortion [15]. The Lambert Equal-Area projections - azimuthal and cylindrical - present the Earth's surface in a less distorted rectangular format. While still employed today [3, 16], it is unable to achieve the distance preservance of Werner's. The Mollweide projection retained areal equivalence while reducing the angular distortion within the interior through its ellipsoidal shape [15]. Unfortunately, distortion is still exhibited along the boundaries and non-uniform across the projection.

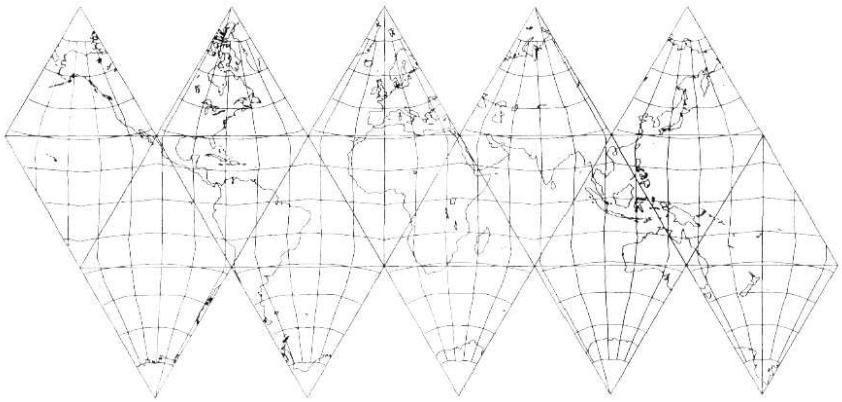

Fig. 2. Icosahedral Mapping Using Snyder Equal Area Projection [14]

As a result of employing a polyhedral surface for his projection, at the expense of a discontinuous flattened map (Figure 2), Snyder [14] was able to reduce the angular distortion due to the polyhedron's close approximation to a sphere. For example, an icosahedron achieves an angular deformation of less than 17.3^o and a scale variation of less than 16.3%. Furthermore, the employment of a polyhedron more readily facilitates its visualization since a polyhedron, or mesh-based, approach is commonly employed within computer visualization.

Alternative approaches have been presented. Leeuwen et al. [10], for example, later demonstrated an alternative equal areal polyhedral projection, more uniformly distributing the angular deformation across the surface. Their Slice and Dice approach is initially constructed comparably to Snyder's, but instead of employing a modified Lambert Azimuthal equal area projection, they partition the surfaces so as to preserve areal ratios. As a result, the distortion is less noticeable, eliminating discontinuities and reducing cusps. Unfortunately, an

inverse projection is neither presented nor readily determined - a necessity for computational visualization.

In order to guarantee a real-time visualization, it is important to discuss what it means for a visualization to be real-time. For an interactive system, which responds readily to an individual's input, a visualization must redraw itself at a minimum rate of 24 frames per second (fps). For 24 fps, this corresponds to 0.04167 seconds of screen time per frame. For items that are drawn on the screen, it then becomes a matter of how many items, and for what intensity of computational processing are we able to achieve within the 0.04167 seconds. A review of the original Snyder inversion process is explored, and the number of inverse calls possible within the 0.04167 seconds is determined.

3 Snyder's Polyhedral Projection

An initial discussion of Snyder's polyhedral projection is presented. This is followed by the inversion and its drawbacks.

3.1 Snyder Projection

Snyder's projection defines a function F mapping the spherical point p and computing its position on the polyhedron. To do so, the Lambert Azimuthal Equal-Area projection is centered upon each of the respective faces. In this Lambert Azimuthal Equal-Area projection, a plane is set tangent to the sphere, and points are projected along radial arcs down to this plane. For the Snyder projection, it must be modified for the polyhedral employment to ensure precise edge matching. F is construct by first decomposing the polyhedral faces into their smallest symmetric region - always a right triangle (Figure 3). Then, the area on the plane and on the sphere are made equivalent through a scaling factor between the radius of the sphere, and the radius of the polyhedron's inscribing sphere. The third step defines a triangle on the polyhedron whose area exactly matches that of a spherical triangle bounded by point P. Finally, the new point P' is positioned along this triangle's edge while maintaining areal scale.

Figure 3 visualizes the triangles and their variables. As illustrated, the main face is divided into three subtriangles, and then further halved into right triangles. Such a division may be applied to any regular polygon, and Snyder includes the equations for alternative sphere-circumscribing polyhedra.

Figure 3 additionally illustrates several angles and vertices used through the projection of point P to point P'. Spherical triangle $\triangle ABC$ and polyhedral triangle $\triangle A'B'C'$ are constructed from the underlying polyhedral face with A, A' the centroids, B, B' the vertices, and C, C' each edge's midpoint. During area preservation, radius R of the spherical polyhedron is associated with radius R' of the sphere circumscribing the polyhedron. D is defined using a great circle arc from A through P, intersecting BC. The resulting $\triangle ABD$, with angles $\angle G$, $\angle H$ and $\angle Az$, determine $\triangle A'B'D'$ with the same area. Angle or azimuth $\angle Az'$ is used to determine $\triangle A'B'D'$, which in turn computes point D'. In the final step,

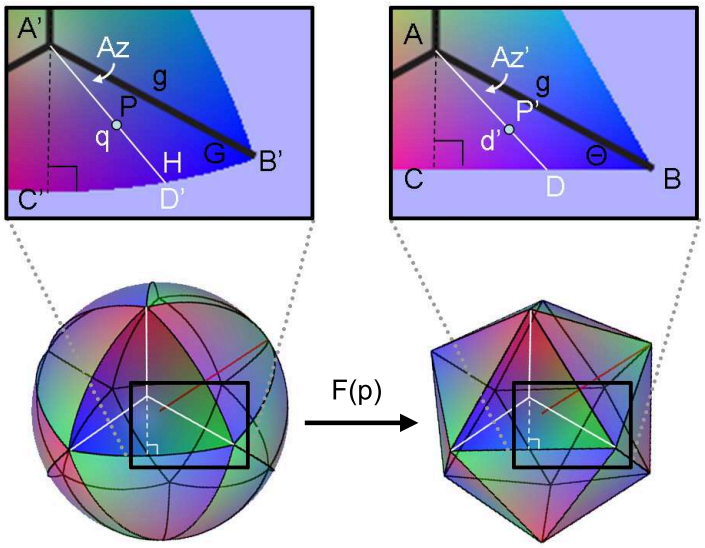

Fig. 3. Spherical and Planar Icosahedron with Symmetric Decomposition (Red line indicates the radius)

the ratios between arc length $q = AD$ and edge length $d' = A'D'$ fix P' in place. It should be noted that angles $\angle\Theta$ and $\angle G$ are fixed for a given polyhedron. These values are listed in Snyder's paper [14].

Having defined these variables, they can then be used to more precisely recreate the Snyder projection. The initial formulation of Snyder's scaling based on the radius R and R' is well discussed by both Snyder [14] and Harrison et al. [7]. The subsequent step ensures the point retains area during throughout the projection, and therefore must position it precisely within the planar triangle. To do so, we must position point D - which may be represented through the calculation of $\angle H$ - from the Spherical Law of Sines and Cosines as follows:

$$\angle H = \arccos(\sin Az \sin G \cos g - \cos Az \cos G), \tag{1}$$

where g is the arclength between AB. Consequently, the area of $\triangle ABD$ is:

$$A_{ABD} = \frac{(Az + G + H - 180^o)\pi R^2}{180^o}. \tag{2}$$

To associate triangle $\triangle A'B'D'$ with its circumscribing radius, and angles of interest, Snyder defines the area as:

$$A_{A'B'D'} = \frac{(R' \tan g)^2 \tan Az'}{2(\tan Az' \cot \Theta + 1)}. \tag{3}$$

Since we need $A_{ABD} = A_{A'B'D'}$, we transform equations 2 and 3 to define our planar azimuth, Az':

$$Az' = \arctan(2A_{ABD}R'^2 \tan^2 g - 2A_{ABD} \cot \Theta).$$

The final step positions point P' along this calculated azimuth, Az' so that it preserves areal scale. The proportionality factor is described in detail by Snyder [14] and Harrison et al. [7]. At this stage, the planar triangle coordinates (x, y) for our projected point is determined.

It should be mentioned that the calculations presented by Snyder are strongly tied to the specific layout of the flattened polyhedron. A visualization of the layout, along with a table of offset coordinates are provided within his paper.

Though this forward projection requires several trigonometric calls, it is otherwise a straightforward closed form.

3.2 Inverse Snyder Projection

The inversion reverses the forward projection, finding the spherical coordinates of P given the coordinates of P' on the polyhedron. From the forward projection, symmetric extraction and radius scaling requires nominal modification. The final reversal of the forward projection - positioning P along great circle arc AD - is also straightforward. The complexity resides within the calculation of Az. In matching the areas of $\triangle ABD$ and $\triangle A'B'D'$, we have Az' and must compute Az. Thus, we can define the area of $\triangle A'B'D'$ as:

$$A_{A'B'D'} = \frac{R'^2 \tan^2 g}{2(\cot Az' + \cot \Theta)}.$$

Setting this equal to the area of $\triangle ABD$, from equation 2, it can be noted that Az is involved linearly and trigonometrically, through the reliance of $\angle H$ on the arccos of $\sin Az$ and $\cos Az$ by equation 1. Solving for Az results in a non-linear equation. Since a closed form is neither proposed nor easily determined, Snyder suggests the Newton-Raphson iterative approach to deduce an adequate value [14]. This approach computes the derivative and uses it to iteratively find an improved approximate solution. Consequently, the following equations are used:

$$g(Az) = \frac{180^o A_{A'B'D'}}{\pi R^2} - G - H - Az + 180^o \tag{4}$$

$$g'(Az) = \frac{\cos Az \sin G \cos g + \sin Az \cos G}{\sin H} - 1 \tag{5}$$

$$\Delta Az = -\frac{g(Az)}{g'(Az)}. \tag{6}$$

On each iteration, ΔAz is added to Az until ΔAz goes below some pre-determined threshold, ϵ.

These calculations are specified in Algorithm 1.

Algorithm 1 Inverse Snyder Calculation

Require: $face$, Az'
  $lat \leftarrow 0$
  $lon \leftarrow 0$
  // Convert Az' to symmetric subregion (not shown)
  // Determine initial estimate for Az
  $Az \leftarrow Az'$
  $A_G \leftarrow \frac{R'^2 \tan^2 g}{\cot Az' + \cot \Theta}$
  $\delta \leftarrow 1$
  // Iterate using Newton-Raphson
  while $\delta > \epsilon, \epsilon \sim 0$ **do**
    $F(Az) \leftarrow \frac{180^o A_G}{\pi R^2} - G - H - Az + 180^o$
    $F'(Az) \leftarrow \frac{\cos Az \sin G \cos g + \sin Az \cos G}{\sin H} - 1$
    $\delta \leftarrow \frac{F(Az)}{F'(Az)}$
    $Az \leftarrow Az + \delta$
  end while
  // Unwrap Az, so it falls in the correct symmetric region of the face (not shown)

Due to the non-linear equation, the inverse projection requires a number of iterations to converge on a value within a required accuracy. Furthermore, computations within the iteration process are often repeated and therefore redundant within a formal implementation. These repetitions have been identified and removed by the previous body of optimization work.

4 Optimizations

With the lack of closed form, and resulting indeterminate iterations required for root-finding, numerous optimizations were applied by Harrison et al. [7], to speed up the process. In a graphical application where inversion calls occur millions of times within a single screen of information, slow implementations impede real-time requirements. While an order of magnitude in reduction is preferred, even a constant reduction is beneficial.

These optimizations continue to be applied to an icosahedron. Application to other sphere circumscribing regular polyhedra is possible, but beyond the focus of the work.

Three types of optimizations were performed: operation reduction, curve fitting and, lastly, iteration removal. The operation reductions employed common computer science approaches, involving the identification and temporary storage of repeated calculations. Furthermore, the simultaneous calculation of sin and

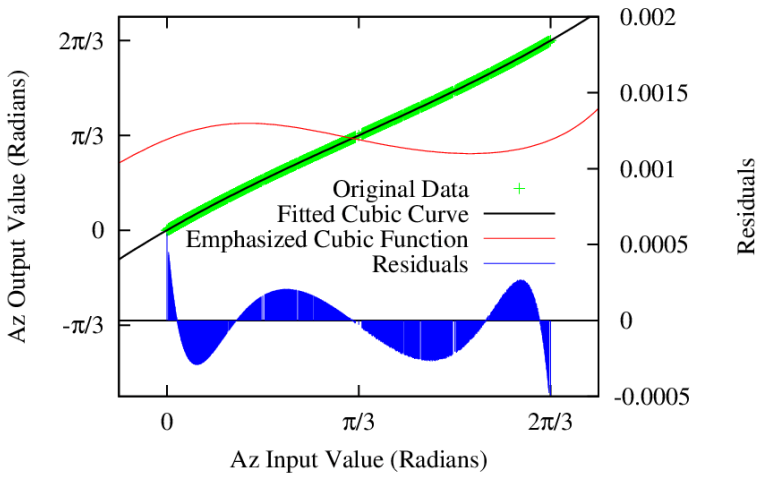

Fig. 4. Azimuth Before Against Azimuth After Iterative Newton Raphson

cos for angles which undergo both processes is improved through *sincos* directives. Such directives are capable of performing both computations in the time it takes to evaluate one separately. The improvements were classified as trivial, and were not, and continue not to be evaluated for improvements in optimization.

The more insightful optimization involved the application of a curve fitting approach. In this way, the Netwon Raphson iterations were initiated with a more reliable estimate. It was observed that the formulae applied to Newton Raphson were entirely dependant upon the input azimuth. When six thousand evenly distributed values within the possible range of the azimuth (up to 60^o on an equilateral icosahedron face) were plotted against Newton Raphson's resulting azimuthal value, a smooth curve was constructed (Figure 4). To emphasize its non-linear form, the exponential of its difference is also plotted: $y = e^{5(f(x)-x)}$.

Consequently the data is well suited for applying a polynomial approximation to for curve fitting. While higher degree polynomials were evaluated for the resulting residuals (against the data, Table 1), only a cubic polynomial was considered for analysis. The assumption was that as the degree of the polynomial increased, the operational requirements would offset the benefits of the improved initial estimate. Within this work, the higher degree polynomials are more thoroughly evaluated, and constructed using Horner's rule [1]. It should be noted that when finding higher degree polynomials, coefficients must be non-zero. For many of the even degree polynomials, this resulted in a close to zero coefficient for the dominant term. The operation count, which is reduced through Horner's rule, is included within Table 1.

This improved estimate, through the use of a cubic approximating polynomial, resulted in a 25% reduction in iterations, and a 15% reduction in computational time. These improvements are possible while still ensuring the solution converges to an accurate value.

Table 1. Polynomial Approximating Azimuthal Shift

Polynomial	Sum of Squares of Residuals	Variance of Residuals	Operation Count
Degree 1	1.19e+00	2.02e-04	2
Degree 2	9.27e-01	1.66e-04	4
Degree 3	2.30e-04	3.92e-08	6
Degree 4	2.06e-04	3.51e-08	8
Degree 5	2.51e-05	4.28e-09	10
Degree 6	2.20e-05	3.75e-09	12
Degree 7	9.06e-07	1.55e-10	14
Degree 8	7.90e-07	1.34e-10	16
Degree 9	4.79e-08	8.18e-12	18
Degree 10	4.61e-08	7.87e-12	20

Upon acquisition of such this improved estimate for the Newton Raphson iterative approach, an evaluation of eliminating iterations entirely was explored. To this end, the result of the polynomial function was directly employed, and its results evaluated. As expected, due to the lack of precision within the framework, positional and areal error was generated, though nominally. The elimination of iterations resulted in a 45% reduction in computational time, at the expense of $0.7km^2$ areal error, and a displacement of 5.9 m. Consequently, for a visualization, or analysis requirement, wherein such errors are negligible for visibility or tolerance, the eliminated approach offers a viable alternative.

5 Supplemental Analysis

Lacking within the analysis of Harrison et al. is the briefly discussed polynomial approximations. While it is assumed that a cubic polynomial is sufficient, evidence is not provided to attest to this situation. As the polynomial improves the estimation of the curve fitted data, it increases the possibility for a reduction in iterations. Furthermore, the additional operational expense, for this improved estimation enables a reduction in errors when iterations are eliminated and the polynomial directly applied.

As such, different polynomial degrees are tested, and evaluated for their ability to support improved estimations. Further evaluation of the resulting real-time support is also explored.

6 Results

Implementation and testing occurred using Qt/C++ on an Intel i7 quad core processor under Ubuntu 10.05.

The original implementation was contrasted against approaches described using a fitted polynomial. Polynomials of degrees one through ten are evaluated. It was observed that a polynomial at degree ten no longer exhibits a time

improvement over the original, and as such, higher degrees are not considered. As with Harrison et al., operation reduction is not considered for comparison. Instead, the reduction of iterations through an improved initial estimate, and the elimination of iterations by full use of the polynomial approximation are evaluated. An error analysis for the latter is also provided.

For each of the three approaches - the original, improved polynomial approximation, and iteration elimination - profiling, using *gprof* (v2.17), was performed 100 times for a high resolution, or quality level. A resolution refers to the number of times an icosahedron face is initially divided prior to vertex projection. For example, the 100×100 resolution level employed for the tests herein will split the face into 10,000 subtriangles. The vertices of these faces are then projected through the respective inversions.

Numerical results are presented in Table 2. The "Method" column indicates the version explored - the original inverse projection, the improved polynomial approximation, or the eliminated iterations variant. The average iteration reflects the improved estimate reducing the iterative convergence. This is also visualized in Figure 5, where the distribution of iterations across the surface of the sphere coloured accordingly. As the approximation improves, it requires less iterations to converge. The percent time improvement compares the improved and eliminated approaches against the original. Iteration improvement over the original is presented for the improved but not the eliminated approach as no iterations occur.

Error analysis for the elimination approach can be found in Table 3. Here, distance is an absolute value, and the average distance converted to metres. Similarly, the average and maximal error - as a percentage - are presented. The average area error is also converted into m^2, based on the surface area of the Earth being 510,072,000 km^2. The distribution of area error is visualized in Figure 6. Blue indicates an increase in area, whereas purple indicates a decrease.

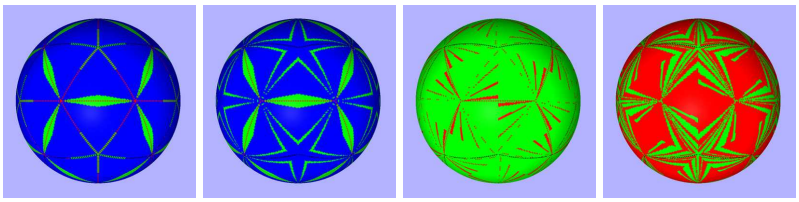

(a) Original (b) Poly. Degree 1 (c) Poly. Degree 5 (d) Poly. Degree 8

Fig. 5. Iteration Distribution. Blue = 4, Green = 3, Red = 2

Analyzing the real-time support for the optimizations involves exploring how many points may be projected within the aforementioned 0.04167 seconds. If we assume that the only time consumption during the duration is the projection of points, we observe - based on the average time per call that approximately 240,000 points may be mapped through the original inverse Snyder projection. If

Table 2. Profiling Results

Poly. Degree	Method	Avg Iter.	Avg Time (s)	Std Dev.	Time Improv.	Iter Improv.
	Original	3.82	0.1019	0.0288		
1	Improved	3.82	0.1003	0.0322	1.57%	0.00%
1	Eliminated	0	0.0531	0.0238	47.89%	
2	Improved	2.75	0.0997	0.0302	0.99%	1.70%
2	Eliminated	0	0.0562	0.0226	44.19%	
3	Improved	2.92	0.0939	0.0323	6.38%	23.56%
3	Eliminated	0	0.0550	0.0203	45.16%	
4	Improved	3.26	0.0963	0.0322	3.51%	14.51%
4	Eliminated	0	0.0579	0.0240	41.98%	
5	Improved	2.89	0.0915	0.0299	7.76%	24.19%
5	Eliminated	0	0.0553	0.0248	44.25%	
6	Improved	2.85	0.0944	0.0334	5.22%	25.43%
6	Eliminated	0	0.0577	0.0251	42.07%	
7	Improved	2.43	0.0854	0.0270	13.12%	36.27%
7	Eliminated	0	0.0579	0.0224	41.10%	
8	Improved	2.31	0.0855	0.0293	15.09%	39.57%
8	Eliminated	0	0.0576	0.0230	42.80%	
9	Improved	2.29	0.0830	0.0258	17.17%	40.13%
9	Eliminated	0	0.0558	0.0240	44.31%	
10	Improved	3.74	0.0999	0.0308	4.31%	1.85%
10	Eliminated	0	0.0580	0.0227	44.44%	

Table 3. Error Analysis of Elimination Approach

Poly. Degree	Avg Dist. Error	Max Dist. Error	Avg Dist. Error (m)	Avg Area Error (%)	Max Area Error (%)	Avg Area Error (m^2)
1	4.856e-03	2.193e-02	3.093e+02	-6.665e-04	9.754e-01	-1.700e+04
2	5.121e-03	3.451e-02	3.262e+02	-7.862e-04	9.690e-01	-2.005e+04
3	9.490e-05	6.193e-04	6.044e+00	1.758e-06	1.596e-02	4.485e+01
4	1.538e-03	1.223e-02	9.796e+01	-4.911e-05	9.876e-01	-1.253e+03
5	2.167e-04	1.640e-03	1.380e+01	2.428e-06	1.596e-01	6.193e+01
6	2.456e-05	2.831e-04	1.564e+00	2.237e-06	7.625e-03	5.705e+01
7	5.709e-06	6.889e-05	3.636e-01	5.883e-07	1.813e-03	1.500e+01
8	4.667e-06	6.842e-05	2.973e-01	7.744e-07	2.302e-03	1.975e+01
9	8.099e-06	7.995e-05	5.158e-01	1.366e-07	7.884e-03	3.485e-02
10	1.717e-01	1.820e+00	1.093e+04	-7.657e+00	7.670e-01	-1.953e+08

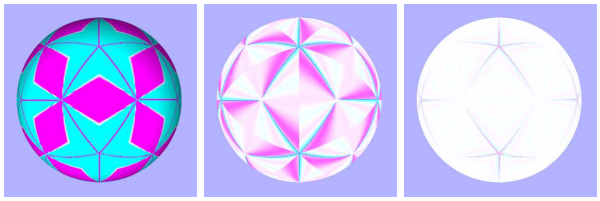

(a) Poly. Degree 1 (b) Poly. Degree 5 (c) Poly. Degree 8

Fig. 6. Eliminated Distortion - Area Change. Blue - growth, Purple - reduction.

we employ the improved iteration technique, this increases to 270,000. Due to the large reduction in time for the eliminated approach, we observe approximately 440,000 points that may be projected in the same time frame. This corresponds to the approximately 44% decrease in computational time. Of course, visualization involves more than just the projection of points, however the values provided represent a maximal potential given the optimizations. The different quantity of points that may be projected are visualized in the graph of Figure 7. The figure illustrates how the decrease in processing time for the iteration elimination approach increases the number of projected points. Further, the number of projected points for the improved approach gradually increases, over the original, as the degree, and consequently, the accuracy of the polynomial improves. This increase reaches a peak when employing a polynomial of degree 9, whereas the additional calculations for degree 10 begin to inhibit the improved approximation thereby reducing the points that may be projected in real-time.

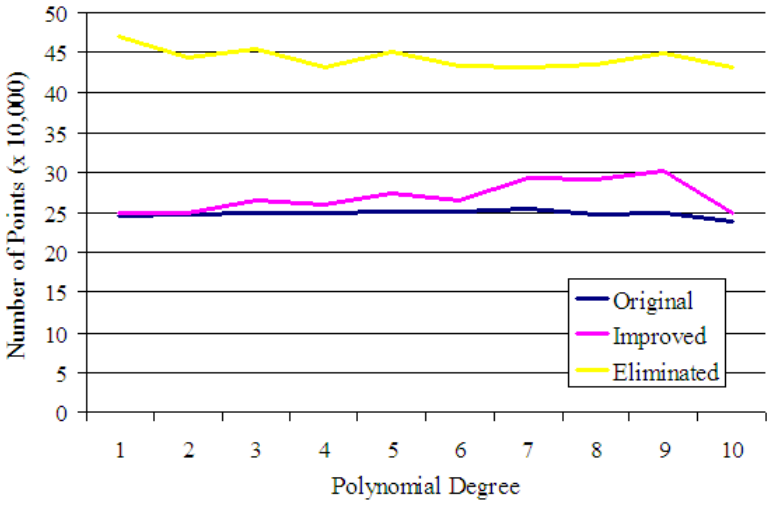

Fig. 7. Number of Points Projected in Real-Time (24 fps)

7 Discussion

Based on the error comparison between the original projection and the eliminated approach, as illustrated in Table 3, distance and areal errors are improved upon as the degree of the approximating polynomial increases. This corresponds to a better approximation for the fitted curve. For example, with a degree of 3, an average area error of 45 m^2 occurs. A polynomial of degree 9, on the other hand, has an average areal error corresponding to 3.5 m^2. This reduction in error increases the resolution upon which the system may employ the faster elimination approach before this error becomes apparent.

The achievement of almost a half a million points, which may be projected within the 24 fps requirement, is a great improvement over the quarter million previously possible. This is particularly important when coupled with a visualization system that exploits level of detail visualization techniques, and therefore have the ability to employ the eliminated approach with simultaneous precision at the high levels of detail.

8 Conclusion

With visualization systems requiring real-time accurate and equal area information of large quantities of data, an effective projection mechanism is imperative. With much data acquired through planar means, area preservation during spherical conversion is important. Such an area preserving quality provides researchers and businesses with accurate analysis of their data. Such analysis, along with the visualization, relies on underlying feature outlines which may span thousands or even millions of points for a single region. The conversion of these feature points to their spherical coordinates requires both accuracy and efficiency. The repeated employment of the inverse Snyder projection, as occurs in industry, can be extremely time consuming - greatly limiting the number of points available for display within a real-time framework. The speeds ups provided by Harrison et al greatly reduce time taken for the iterative root-finding for the non-linear calculations, however an improved approximating polynomial is able to further improve these results.

Whereas Harrison et al found a 25% iteration reduction with a cubic polynomial, upwards of 40% is possible with a degree 9. Furthermore, while the higher degree doesn't significantly improve the speed of the eliminated iteration approach - roughly 45% - it reduces the error ten fold. This improvement increases the amount of data that may be visualized until this erroneous threshold is reached.

Finally, the real-time qualities of these optimizations are obvious and demonstrate the need for their employment. Whereas the original Snyder inversion only supported a quarter million points for projection, the optimized elimination approach supports almost one half million points. This increase in visualization data lends itself to improved visualization, processing and analysis time.

If we consider the Earth as a perfect sphere, it remains of worth to expand on this work further by analyzing the different sphere circumscribing polyhedron.

Snyder discovered his projection resulted in the least amount of distortion when projecting with the truncated icosahedron. While the hexagons constructed are challenging to incorporate into a computer graphics visualization, it may be of worth to attempt to work around them to support a representation with reduced shape distortion. In the meanwhile, icosahedral support is employed within industrial applications, and we have demonstrated further optimizations which will benefit the community.

Acknowledgment

This work has been partially supported by PYXIS Innovation and NSERC. We would like to thank Idan Shatz for his thoughtful discussions.

References

1. Borwein, P., Erdlyi, T.: Polynomials and Polynomial Inequalities, pp. 8, 29–41. Springer-Verlag, New York, NY (1995)
2. Canters, F.: Small-Scale Map Projection Design. Taylor & Francis, NY, NY (2002)
3. Commission for Environmental Cooperation: North America. `http://atlas.nrcan.gc.ca/site/english/maps/archives/various/north_america_cec` (2004), [Online; accessed 01-May-2011]
4. Google: Google Earth. `http://www.google.com/earth/index.html` (2011), [Online; accessed 20-November-2011]
5. Google - Imagery: Google Maps. `http://maps.google.ca` (2010), [Online; accessed 11-December-2010]
6. Gore, A.: The Digital Earth: Understanding our Planet in the 21st Century. California Science Center. Los Angeles, USA, 31 (Jan 1998)
7. Harrison, E., Mahdavi-Amiri, A., Samavati, F.: Optimization of Snyder's Inverse Polyhedral Projection. In: Intl. Conference on CyberWorlds. pp. 1–8. IEEE (2011)
8. Kimerling, A.J., Sahr, K., White, D., Song, L.: Comparing Geometrical Properties of Global Grids. Cartography and Geographic Information Science 26(4), 271–288 (October 1999)
9. Lambert, J.H.: Anmerkungen und Zustze zur Entwerfung der Land- und Himmelscharten. Mit 21 Textfiguren (1772)
10. van Leeuwen, D., Strebe, D.: A Slice-and-Dice Approach to Area Equivalence in Polyhedral Map Projections. Cartography and Geographic Information Science 33(4), 269–286 (2006)
11. NASA: Blue Marble. `http://visibleearth.nasa.gov/` (2000), [Online; accessed 11-December-2010]
12. PYXIS Innovation Inc: How PYXIS Works. `http://www.pyxisinnovation.com/pyxwiki` (2011), [Online; accessed 01-May-2011]
13. Snyder, J.P.: Map Projections - A Working Manual: U.S. Geological Survey Professional Paper 1396. U.S. Government Printing Office, Washington, DC (1987)
14. Snyder, J.P.: An Equal-Area Map Projection for Polyhedral Globes. Cartographica 29(1), 10–21 (Spring 1992)
15. Snyder, J.P.: Flattening the Earth: Two Thousand Years of Map Projections. University of Chicago Press, Chicago, Illinois, USA (1997)

16. United States Department of the Interior: Map Projections: From Spherical Earth to Flat Map. http://www.nationalatlas.gov/articles/mapping/a_projections.html (2011), [Online; accessed 01-May-2011]